Photochemistry and Photobiology, 1996, 63(5): 621–627

Optically Pumped Chemiluminescence of Indole-3-Acetic Acid

Sergey N. Krylov* **and Svetlana M. Krylova**

Laboratory of Laser Photobiology and Photomedicine, Institute for Nuclear Physics, Moscow State University, Moscow, Russia

Received 14 August 1995; accepted 26 January 1996

ABSTRACT

Optically pumped chemiluminescence of indole-3-acetic acid (IAA) was observed and studied. Rose Bengal (RB) was used as a photosensitizer. Long-lived chemiluminescence (CL) appeared after irradiation of the IAA/RB reaction mixture by monochromatic light at 550 nm (the maximum of RB absorption) or by visible light. The CL spectrum had a maximum at 480 nm. The kinetics of the CL decay were single exponential. Single-exponential kinetics were characterized by two experimentally measured values: initial CL intensity and exponential lifetime of the CL decay. We studied the influence of five parameters: (1) the rate of irradiation fluence, (2) the time of irradiation, (3) RB concentration, (4) IAA concentration and (5) buffer pH on the initial CL intensity and the CL lifetime. Initial CL intensity was proportional to the rate of irradiation fluence and the concentration of RB. Saturation was observed in dependencies of initial CL intensity on the time of irradiation, the concentration of IAA and the buffer pH. The lifetime of the CL decay decreased with increasing pH and did not depend on the other four parameters. The mechanism explaining the experimental results was suggested and detailed kinetic analysis was performed to prove the proposed mechanism. Quantum yield of the CL and five rate constants that are involved in the mechanism were determined.

INTRODUCTION

Optically pumped chemiluminescence (CL)† was first demonstrated by Kuschnir and Kuwana who observed the blue emission during irradiation of the basic water solution of xanthene dyes and luminol (1). They suggested the CL was the result of the reaction of a singlet oxygen with luminol. Matheson and Lee have performed a kinetic analysis of the dye-sensitized CL of luminol on the basis of this hypothesis (2). However, later they had shown that singlet oxygen was not involved in the reaction contributing to the CL (3). They suggested that type I photosensitized luminol oxidation is the main source of luminol CL. Recently, Motsenbocker *et al.* (4) have shown that the CL resulting from the dye-sensitized photooxidation of luminol is a prospective technique for the creation of a new chemiluminescent diagnostic method. They introduced the term "optically pumped chemiluminescence." That technique does not require enzyme nor separate oxidants such as hydrogen peroxide for the chemiluminescent reaction. The catalysts of optically pumped CL are more stable and less temperature sensitive than exzymatic catalysts. Thus, optically pumped CL can compete with enzyme techniques when reagent stability is the most important parameter.

Indole-3-acetic acid (IAA) is a natural phytohormone with many growth regulatory functions (5). The level of IAA *in vivo* is controlled particularly through its oxidation by peroxidases and photooxidation (6). Peroxidase-catalyzed oxidation of IAA utilizes oxygen rather than hydrogen peroxide in a very complex process. Peroxidase is converted from the native form to several catalytic and inactive species (7). Many intermediates and final products of IAA are formed during the reaction (8). The overall reaction exhibits a variety of nonlinear dynamics (9–11). At neutral pH peroxidase-catalyzed oxidation of IAA goes through the peroxidase pathway accompanied by a free radical chain reaction (12). The peroxidase cycle generates free radicals required for propagation of a free radical chain reaction, whereas a free radical chain reaction produces organic hydroperoxide, which is needed for the initiation of the peroxidase cycle. The formation of the IAA radical cation, indole-3-methyl radical (scatol radical), indole-3-methylperoxy radical and superoxide radical were observed (8,13–16). Hydroperoxide formed in a free radical chain reaction is unstable and multiple attempts to isolate and characterize this substance failed (17,18).

Photooxidation of IAA is proposed to be responsible for plant phototropism (5). The oxidation of IAA *in vivo* proceeds through photosensitization by biological pigments. Therefore the mechanisms of sensitized oxidation of IAA and other indoles were studied *in vitro* (19,20). It was shown that both photooxidation type I and photooxidation type II were involved in IAA photodegradation and the rate of photoreaction depended on pH.

Indole-3-acetic acid is a known chemiluminescent substrate (5). Peroxidase-catalyzed aerobic oxidation of IAA results in the emission of light at 420, 465 and 535 nm (24,25). The CL is considerably enhanced by the addition of xanthene dyes. It was proposed for many years that the enhance-

*To whom correspondence should be addressed at: Department of Chemistry, University of Alberta, Edmonton, Alberta T6G 2G2, Canada. Fax: 403-492-8231;
e-mail: skrylov@gpu.srv.ualberta.ca.

†*Abbreviations*: CL, chemiluminescence; IAA, indole-3-acetic acid; RB, Rose Bengal.

 $5.00+0.00

ment was due to energy transfer from enzyme-generated electronically excited species to xanthene dyes (21,22). Recent studies however have shown that the enhancement of the CL was the result of peroxidase-mediated co-oxidation of xanthene dyes and IAA rather than energy transfer (8,23). In our previous paper we reported that phenol-inhibited peroxidase-catalyzed IAA oxidation was reinitiated by light in the presence of the photosensitizer Rose Bengal (RB) (9). Here we present, for the first time, a study of the optically pumped CL of IAA. Rose Bengal was used as a photosensitizer. Kinetic analysis was performed in order to examine the proposed mechanism of the reaction and to determine the reaction rate constants and quantum yield of the CL.

MATERIALS AND METHODS

Materials. The IAA, RB and buffer components were obtained from Sigma (St. Louis, MO, USA). All solutions were prepared using triple distilled deionized water: 0.1 *M* citrate-phosphate, phosphate, tris and carbonate–bicarbonate buffers were used for pH regions 4.0–5.5, 6.1–7.8, 8.2–9.0 and 9.6–10.0, respectively. Except where otherwise stated the standard reaction mixture contained 1 *mM* IAA and 3.3×10^{-7} *M* RB in phosphate buffer, pH 7.4. Final volume of the reaction mixture was 3 mL. The temperature was kept at 25 ± 0.5° C. Standard conditions of irradiation are described below.

Methods. The kinetics and spectra of optically pumped CL were followed with a specially designed chemiluminometer. A quartz cuvette (30 mm diameter) containing the reaction mixture was located above a photocathode of the photomultiplier. Thus, the CL was detected through the bottom of a cuvette. A photomultiplier FEU-130 with measured spectral sensitivity in the 200–650 nm region was operated in the photon-counting mode. After the irradiation source was turned off, a shutter, protecting the photomultiplier from irradiation by exciting light, was immediately opened and the measurements were started.

For spectral measurements a set of optical cut-off filters was placed between the bottom of the cuvette and the photocathode. Standard glass filters and liquid filters containing potassium chromate and bichromate solutions were utilized. Liquid filters in the 450–550 nm region were used because of an intense self-emission from standard glass filters.

The impulses of the photomultiplier were registered and counted by a multichannel analyzer LP 4900 B (Afora, USA). A microprocessor device provided the possibility of carrying out programmable measurements and automatic changing of filters as well as experimental data processing.

The CL spectra were obtained by differentiation of the integral spectrum measured through the cut-off filters. In order to obtain real spectra we made corrections for the change of the CL intensity during the measurement, spectral sensitivity of the photomultiplier, the spectra of the cut-off filter transmission and the intensity of filter self-phosphorescence.

Absolute quantum sensitivity of the photomultiplier at the wavelength of the CL (around 480 nm) was about 10%. Approximately 35% of the isotropically emitted CL reached the photocathode. So, in order to calculate absolute quantity of emitted CL quanta we multiplied the quantity of registered quanta by the factor $(0.035)^{-1}$.

The source of white light, OVS-1, and an optic fiber conductor were used for the reaction mixture irradiation. We verified the intensity of irradiation by means of a diaphragm. The rate of irradiation fluence I_{IRR} integrated over the spectrum was measured with a radiometer/photometer EG&G (USA). The relative spectrum of the irradiation $J_{REL}(\lambda)$ was measured with an optical spectral analyzer WP-4 (B&M Spectronic, Germany). The absolute spectrum of the irradiation was calculated according to the expression

$$J(\lambda) = J_{REL}(\lambda)\frac{I_{IRR}}{\int_{\lambda_{min}}^{\lambda_{max}} I_{REL}(\lambda)\, d\lambda} \qquad (1)$$

where λ_{min} = 400 nm and λ_{max} = 800 nm are lower and upper limits

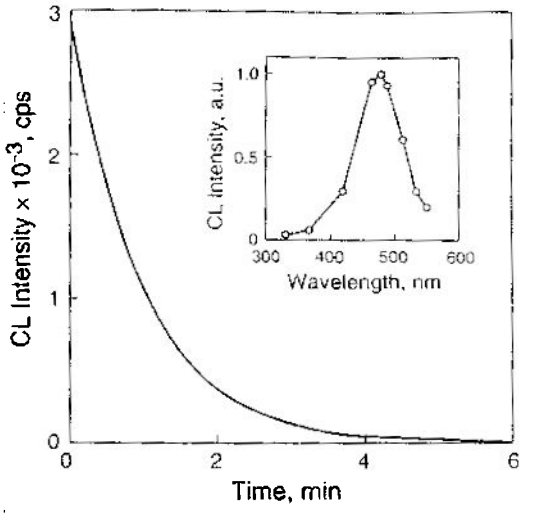

Figure 1. Chemiluminescence decay after the light source is turned off. Insert shows the spectrum of the CL. Experimental conditions are 1 m*M* IAA and 3.3×10^{-7} *M* RB in phosphate buffer pH 7.4, final volume 3 mL, temperature 25 ± 0.5°C, the rate of irradiation fluence 3.56×10^{-4} mol m^{-2} s^{-1} and the time of irradiation 30 s.

of WR-4 sensitivity. The overlap integral between the spectrum of RB absorption and spectrum of irradiation was calculated as

$$\int_{\lambda_{min}}^{\lambda_{max}} \epsilon(\lambda) J(\lambda)\, d\lambda \qquad (2)$$

where $\epsilon(\lambda)$ is an extinction coefficient of RB.

Except where otherwise stated standard conditions of irradiation were as follows: the rate of irradiation fluence (I_{IRR}), 3.56×10^{-4} mol m^{-2} s^{-1} and the time of irradiation (t_{IRR}), 30 s. The overlap integral corresponding to that fluence rate was calculated using Eq. 2: 3.91×10^{-1} s^{-1}.

A monochromator was attached to the irradiation source for the production of 550 nm monochromatic light (a maximum of RB absorption) when it was required. Standard software for nonlinear regression "Enzfitter" was used for k_3 determination. Experimental data I_{CL}^{∞} *vs* [IAA] (Fig. 3B) were fitted by the function

$$I_{CL}^{\infty} = \text{const}/(k_2 - k_3\,[\text{IAA}]).$$

RESULTS AND DISCUSSION

Experimental results

If the mixture IAA/RB was irradiated by 550 nm monochromatic light (the maximum of RB absorption) or visible light, then long-lived luminescence was observed after the light source was turned off (Fig. 1). The luminescence decay curve was a single exponential. This meant that the process resulting in light emission was unimolecular or quasiunimolecular. The exponential lifetime of the emission was equal to 1 min under standard irradiation conditions (see Fig. 1), which is much more than the fluorescence or even phosphorescence lifetime. This suggests that light emission appeared due to an optically pumped chemical reaction. Moreover, the maximum of the luminescence spectrum was at 480 nm (Fig. 1, insert). This wavelength is shorter than the wavelength of irradiating monochromatic light. Thus, this affords additional proof that this is a photochemical reaction rather than phosphorescence or fluorescence. We suggest that the main emitting product is the same as one of the products of peroxidase-catalyzed IAA oxidation, which emits at 465 nm

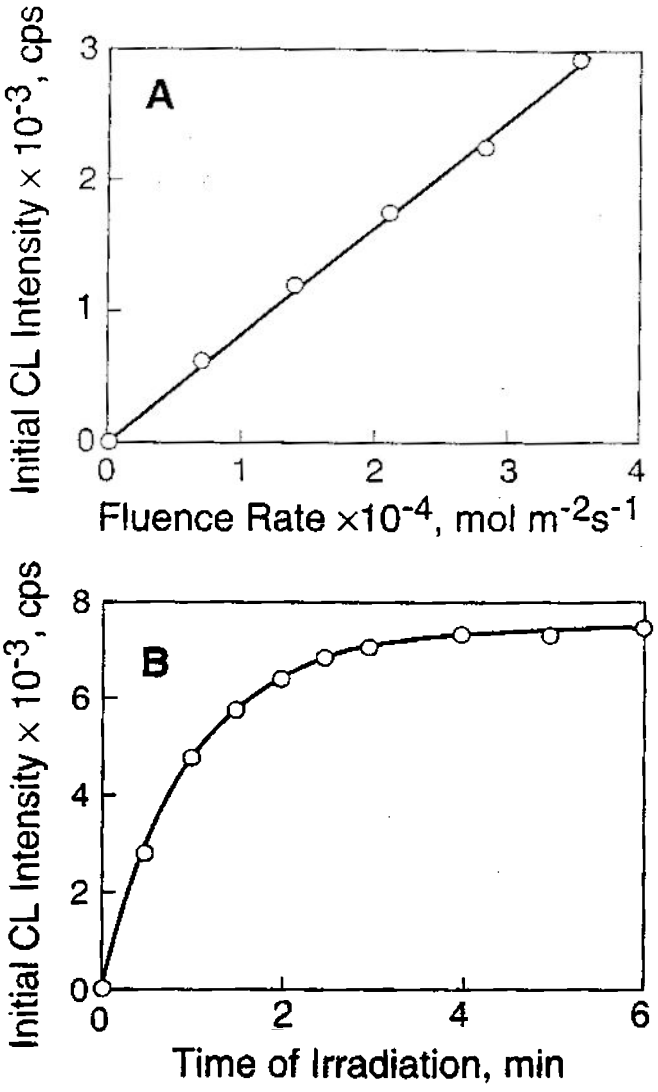

Figure 2. Initial intensity of the CL, after the light source is turned off, as a function of the rate of irradiation fluence (A) and the time of irradiation (B). Except for the parameters that are variables, the experimental conditions are 1 m*M*IAA and 3.3×10^{-7} *M* RB in phosphate buffer pH 7.4, final volume 3 mL, temperature 25 ± 0.5°C, the rate of irradiation fluence 3.56×10^{-4} mol m^{-2} s^{-1} and the time of irradiation 30 s.

(24,25). The nature of the optically pumped luminescence in the IAA/RB system seemed to be identical to that of the optically pumped CL in the luminol/methylene blue mixture (2–4).

We have already mentioned that the decay of optically pumped CL of IAA was a single exponential that corresponds to a unimolecular or quasiunimolecular reaction. It is obvious that a chemiluminescent chemical reaction is quasiunimolecular rather than unimolecular. Quasiunimolecular CL decay (as well as unimolecular decay) can be completely characterized by two parameters: the initial intensity of the CL (I^0_{CL}) and the exponential lifetime of the CL (τ).

First, we studied the effect of the irradiation fluence rate (I_{IRR}) and the time of irradiation (t_{IRR}) on I^0_{CL} and τ. The I^0_{CL} was proportional to I_{IRR} and increased up to saturation with increasing t_{IRR} (Fig. 2). There was no effect of I_{IRR} and t_{IRR} on τ (not shown).

Further we studied the effect of RB and IAA concentrations on I^0_{CL} and τ. The I^0_{CL} was proportional to [RB] and increased up to saturation with increasing [IAA] (Fig. 3). There was no effect of [RB] and [IAA] on τ (not shown).

Finally, we studied the effect of buffer pH on I^0_{CL} and τ. The I^0_{CL} increased with increasing pH up to saturation, whereas τ decreased with increasing pH (Fig. 4). The concentration of hydroxide anion (OH^-) increases with pH. Therefore, the increase of I^0_{CL} and decrease of τ with increasing pH allow us to suggest that OH^- takes part in the chemiluminescent reaction (2). For the kinetic analysis we use OH^- concentration rather than pH. It should be noted that at low pH (<6) the rate of the CL decay (dI_{CL}/dt) was not a constant during the lumi-

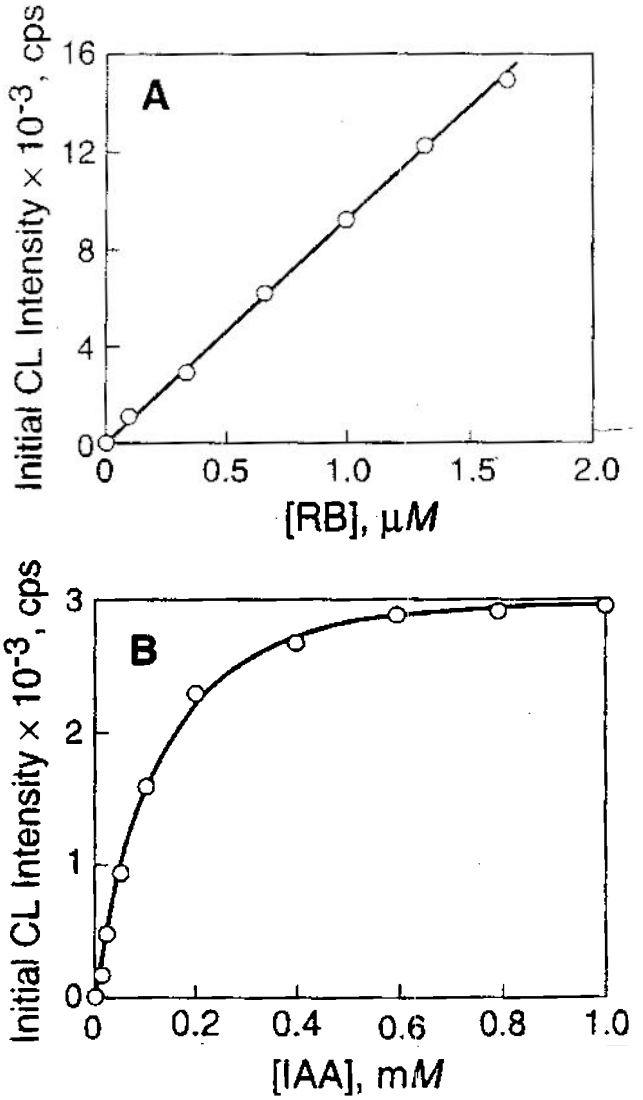

Figure 3. Initial intensity of the CL, after the light source is turned off, as a function of RB concentration (A) and IAA concentration (B). Except for the parameters that are variables, the experimental conditions and 1 m*M*IAA and 3.3×10^{-7} *M* RB in phosphate buffer pH 7.4, final volume 3 mL, temperature 25 ± 0.5°C, the rate of irradiation fluence 3.56×10^{-4} mol m^{-2} s^{-1} and the time of irradiation 30 s.

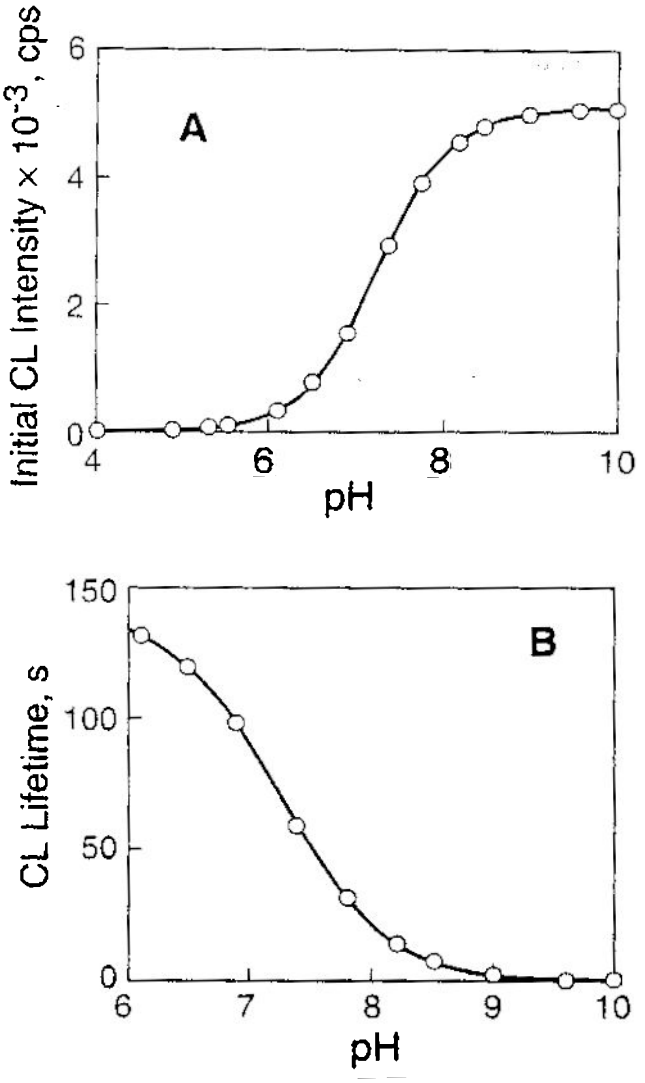

Figure 4. The effect of pH on (A) the initial intensity of the CL, after the light source is turned off, and (B) the single exponential lifetime of the CL. Except for the pH value, which is a variable, the experimental conditions are 1 m*M* IAA and 3.3×10^{-7} *M* RB, final volume 3 mL, temperature 25 ± 0.5°C, the rate of irradiation fluence 3.56×10^{-4} mol m^{-2} s^{-1} and the time of irradiation 30 s.

nescence kinetics. The rate was faster for the initial stages of decay and slower for the tail of the decay. Thus, at low pH the curve for CL decay did not obey pseudo-first-order kinetics. Therefore, Fig. 4B does not show τ for pH < 6.

Kinetic analysis

Two possible mechanisms. The fact that I^0_{CL} is proportional to I_{IRR} and [RB] (see Figs. 2A and 3A) indicates that excitation of RB is the initial step of the photochemical reaction. The saturation in the dependencies I^0_{CL} *vs* [IAA] and I^0_{CL} *vs* pH (see Figs. 3B and 4A) allows us to suppose that IAA and OH^- interact with intermediates of the photochemical reaction. But we do not know in which order IAA or OH^- participate in the reaction. Therefore, we suggest two preliminary mechanisms for kinetic analysis.

Mechanism 1:

$$RB \xrightarrow[h\nu]{k_1} {}^1RB \xrightarrow[IAA]{k_3} X \xrightarrow[OH^-]{k_5,\ \varphi} light$$

$$\downarrow k_2 \text{ quenching} \qquad \downarrow k_4 \text{ deactivation}$$

Mechanism 2:

$$RB \xrightarrow[h\nu]{k_1} {}^1RB \xrightarrow[OH^-]{k_3} X \xrightarrow[IAA]{k_5,\ \varphi} light$$

$$\downarrow k_2 \text{ quenching} \qquad \downarrow k_4 \text{ deactivation}$$

where ^1RB is a triplet excited state of RB, X is the unknown intermediate of the photochemical reaction, which is probably free radical in nature, and ϕ the quantum yield of the CL.

According to mechanisms 1 and 2 the intensities of the CL are, respectively,

$$I_{CL} = \varphi k_5[X][OH^-]V \tag{3a}$$

and

$$I_{CL} = \varphi k_5[X][IAA]V \tag{3b}$$

where V is the volume of reaction mixture.

Steady-state analysis. First we analyze the reaction in its steady state. The concentrations of both the intermediates ^1RB and X are constants in the steady state. Using the condition that $d[^1RB]/dt = 0$ we determined the steady-state concentration of ^1RB for mechanisms 1 and 2, respectively, as

$$[^1RB] = \frac{k_1[RB]I_{IRR}}{k_2 + k_3[IAA]} \tag{4a}$$

and

$$[^1RB] = \frac{k_1[RB]I_{IRR}}{k_2 + k_3[OH^-]}. \tag{4b}$$

Using the condition $d[X]/dt = 0$ we determined the steady-state concentration of X for mechanisms 1 and 2, respectively, as

$$[X] = \frac{k_3[^1RB][IAA]}{k_4 + k_5[OH^-]} \tag{5a}$$

and

$$[X] = \frac{k_3[^1RB][OH^-]}{k_4 + k_5[IAA]} \tag{5b}$$

The intensity of the CL in the steady state corresponds to the experimentally measured initial intensity of the CL I^0_{CL} after the source of light was turned off and when the time of irradiation was saturating (see Fig. 2B). Using Eqs. 3, 4 and 5 we can get the initial intensity of the CL for mechanisms 1 and 2, respectively, as

$$I^0_{CL} = \frac{\varphi k_1 k_3 k_5 I_{IRR}[RB][IAA][OH^-]V}{(k_4 + k_5[OH^-])(k_2 + k_3[IAA])} \tag{6a}$$

and

$$I^0_{CL} = \frac{\varphi k_1 k_3 k_5 I_{IRR}[RB][IAA][OH^-]V}{(k_2 + k_3[OH^-])(k_4 + k_5[IAA])}. \tag{6b}$$

Expressions 6a and 6b are similar except for the location of the coefficients k_2, k_3, k_4 and k_5 in the denominator. Both of the expressions 6a and 6b describe the experimentally determined proportionality of I^0_{CL} to I_{IRR} and [RB] (see Figs. 2A and 3A), as well as saturation in the dependencies I^0_{CL} *vs* [IAA] and I^0_{CL} *vs* [OH^-] (see Figs. 3B and 4A). On the other hand, both of them do not include t_{IRR} and τ as parameters. Therefore, Eqs. 6a and 6b do not allow us to answer the question which mechanism (1 or 2) is correct. In order to answer that question we studied the presteady state of the photochemical reaction and the kinetics of the CL decay.

Presteady-state analysis

According to mechanism 1 the rate of change of X is

$$d[X]/dt = k_3[^3RB]\,[IAA] - (k_4 + k_5[OH^-])\,[X] \quad (7)$$

We integrate this equation with respect to [X] from 0 to $[X]_0$ and with respect to t from 0 to t_{IRR}

$$\int_0^{[X]_0} \frac{d[X]}{k_3[^3RB][IAA] - (k_4 + k_5[OH^-])[X]} = \int_0^{t_{IRR}} dt \quad (8)$$

where $[X]_0$ is the concentration of X at time t_{IRR}. The integration of Eq. 8 provides, upon rearrangement

$$[X]_0 = \frac{k_3[^3RB][IAA]}{k_4 + k_5[OH^-]}\{1 - e^{-t_{IRR}(k_4 + k_5[OH^-])}\} \quad (9)$$

The main quencher of ^3RB in air-saturated solutions is molecular oxygen. The lifetime of ^3RB in the presence of O_2 is determined by the Stern–Volmer equation

$$\tau_{RB} = \frac{\tau^0_{RB}}{1 + \tau^0_{RB}k_q[O_2]} \quad (10)$$

where τ_{RB} and τ^0_{RB} are ^3RB lifetimes in the presence of O_2 and without O_2, respectively, and k_q is the bimolecular rate constant of ^3RB quenching by O_2. The product of $k_q[O_2]$ can be estimated as $2.5 \times 10^5\ s^{-1}$ (see the section Determination of the rate constants and quantum yield of the CL). Therefore, τ_{RB} is less than 10^{-5} s (independently on τ^0_{RB}). The lifetime of the CL under standard conditions is 1 min (see Fig. 1). Therefore, we can assume that in the time scale of CL the concentration of ^3RB is constant, that is $d[^3RB]/dt = 0$. Therefore Eq. 4a can be used in the analysis of the presteady state of the chemiluminescent reaction. Applying 4a to 9 we obtain

$$[X]_0 = \frac{k_1k_3I_{IRR}[RB][IAA]}{(k_4 + k_5[OH^-])(k_2 + k_3[IAA])}\{1 - e^{-t_{IRR}(k_4 + k_5[OH^-])}\} \quad (11)$$

Then applying 11 to 3a we can get the initial intensity of the CL as a function of t_{IRR} for mechanism 1 as

$$I^0_{CL} = \frac{\varphi k_1k_3k_5I_{IRR}[RB][IAA][OH^-]V}{(k_4 + k_5[OH^-])(k_2 + k_3[IAA])}\{1 - e^{-t_{IRR}(k_4 + k_5[OH^-])}\}. \quad (12a)$$

A similar approach allows us to obtain the corresponding expression for mechanism 2 as

$$I^0_{CL} = \frac{\varphi k_1k_3k_5I_{IRR}[RB][IAA][OH^-]V}{(k_2 + k_3[OH^-])(k_4 + k_5[IAA])}\{1 + e^{-t_{IRR}(k_4 + k_5[IAA])}\}. \quad (12b)$$

Both expressions 12a and 12b describe experimentally observed saturation in the dependence of I^0_{CL} *vs* t_{IRR} (see Fig. 2B) although they still do not permit determination of which mechanism is correct.

Analysis of the CL decay. In order to describe the kinetics of the CL decay after the source of irradiation was turned off we have to analyze the kinetic equation for X under the condition $I_{IRR} = 0$ and assume $[^3RB] = 0$. This assumption is based on the fact that the lifetime of ^3RB in O_2-containing solutions is less than 10^{-5}s. This is much less than the lifetime of the CL (see section Presteady-state analysis).

Taking into account the mentioned assumption, we can determine the rate of X decay for mechanism 1 as

$$\frac{d[X]}{dt} = -(k_4 + k_5[OH^-])[X]. \quad (13)$$

We integrate this equation with respect to [X] from $[X]_0$ to [X] and with respect to t from 0 to t

$$-\int_{[X]_0}^{[X]} \frac{d[X]}{(k_4 + k_5[OH^-])[X]} = \int_0^t dt \quad (14)$$

where $[X]_0$ and [X] are the concentrations of X at the end of the irradiation and at the current time t respectively. The integration of Eq. 14 provides, upon rearrangement

$$[X] = [X]_0e^{-t(k_4 + k_5[OH^-])}. \quad (15)$$

Using 15, 11 and 3a we obtain the equation describing the kinetics of the CL decay for mechanism 1 as

$$I_{CL}(t) = \frac{\varphi k_1k_3k_5I_{IRR}[RB][IAA][OH^-]V}{(k_4 + k_5[OH^-])(k_2 + k_3[IAA])} \cdot \{1 - e^{-t_{IRR}(k_4 + k_5[OH^-])}\}e^{-t(k_4 + k_5[OH^-])}. \quad (16a)$$

Using the same approach we can obtain an identical expression for mechanism 2 as

$$I_{CL}(t) = \frac{\varphi k_1k_3k_5I_{IRR}[RB][IAA][OH^-]V}{(k_2 + k_3[OH^-])(k_4 + k_5[IAA])} \cdot \{1 - e^{-t_{IRR}(k_4 + k_5[IAA])}\}e^{-t(k_4 + k_5[IAA])}. \quad (16b)$$

The analysis of Eqs. 16a and 16b allows us to separate the true mechanism from the two possible ones. Indeed, according to Eq. 16a, which corresponds to mechanism 1, the lifetime of the CL decay is $\tau = (k_4 + k_5[OH^-])^{-1}$. The lifetime decreases with increasing [OH^-] and does not depend on the other parameters. This is consistent with our experimental results (see Fig. 4B). According to Eq. 16b the lifetime of the CL decay is $\tau = (k_4 + k_5[IAA])^{-1}$. This is inconsistent with the mentioned experimental facts. Therefore, we accept mechanism 1 as the true mechanism because it is consistent with all of the available experimental results and reject mechanism 2.

Determination of the rate constants and quantum yield of the CL. In our kinetic analysis we used an expression with a formal rate constant of k_1 for the rate of triplet dye formation

$$\frac{d[^3RB]}{dt} = k_1I_{IRR}[RB] \quad (17)$$

whereas the expression for $d[^3RB]/dt$, which contains the real physical parameters is the following

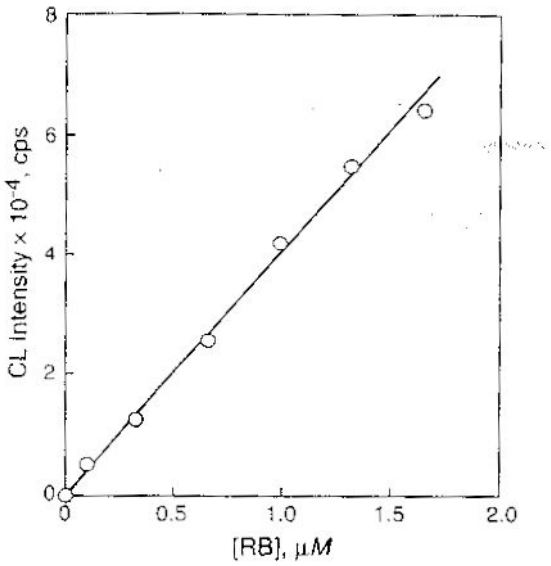

Figure 5. Initial intensity of the CL, after the light source is turned off, as a function of RB concentration. The concentrations of IAA, OH^- as well as the time of irradiation are saturating (see Figs 3B, 4A): [IAA] = 1 m*M*, pH 10, t_{IRR} = 6 min. Final volume of the reaction mixture is 3 mL. The rate of irradiation fluence is 3.56×10^{-4} mol m^{-2} s^{-1}.

$$\frac{d[^3RB]}{dt} = \xi[RB]\int_{\lambda_{min}}^{\lambda_{max}} \epsilon(\lambda)J(\lambda)\,d\lambda \qquad (18)$$

where ξ is an efficiency of intersystem crossing from singlet to triplet excited RB, the overlap integral as described in the Materials and Methods. Using Eqs. 17 and 18 we can calculate k_1 to be

$$k_1 = \frac{\xi\int_{\lambda_{min}}^{\lambda_{max}} \epsilon(\lambda)J(\lambda)\,d\lambda}{I_{IRR}} \qquad (19)$$

For the calculation of the efficiency of intersystem crossing we used the known value of the quantum yield of RB triplet state generation $\xi = 0.8$ (26). The I_{IRR} was measured and the overlap integral was calculated (see Materials and Methods). Using 19 we calculated $k_1 = 8.79 \times 10^3\ M^{-1}\ cm^{-1}$. It should be noted that k_1 has the same dimensional relationship as an extinction.

The rate constant k_2 is actually the rate of ^{3}RB decay in the absence of IAA. The main quencher of triplet excited species in oxygen-containing solutions is molecular oxygen. The concentration of oxygen in aqueous solutions under the condition of air saturation at 25°C is approximately $[O_2] = 2.5 \times 10^{-4}\ M$ (27), whereas the rate of the quenching of xanthene dyes by oxygen is approximately 1/9 of the diffusion-controlled limit, which is approximately $k_q = 10^9\ M^{-1}\ s^{-1}$ (26). So, the pseudo-first-order rate constant for ^{3}RB decay is $k_2 = k_q[O_2] = 2.5 \times 10^5\ s^{-1}$.

According to Eq. 12a under saturating [IAA], $[OH^-]$ and I_{IRR} the initial intensity of the CL is

$$I_{CL} = \varphi\, k_1 I_{IRR}[RB]V \qquad (20)$$

Using this expression we can determine $\varphi k_1 I_{IRR} V$ as a slope α of the strict line I_{CL} *vs* [RB] and consequently the quantum yield can be calculated as $\varphi = \alpha/(k_1 I_{IRR} V)$. The slope determined from the data in Fig. 5 was $\alpha = 1.8 \times 10^{-15}\ m^3\ s^{-1}$ and the quantum yield was calculated to be $\varphi = 1.9 \times 10^{-9}$.

From Eq. 16a, $k_2 - k_3[IAA]_{\nu_2} = 0$, where $[IAA]_{\nu_2}$ is the half-saturating IAA concentration. Thus, $[IAA]_{\nu_2}$ was determined from Fig. 3B as $[IAA]_{\nu_2} = 10^{-4}\ M$. Knowledge of k_2 and $[IAA]_{\nu_2}$ allows us to determine the rate constant k_3: $k_3 = k_2/[IAA]_{\nu_2} = 2.5 \times 10^9\ M^{-1}\ s^{-1}$. The value of k_3 was also determined using nonlinear regression of the data from Fig. 3B (see section Materials and Methods) yielding the same result. Equation 16a shows that

$$k_4 - k_5[OH^-]_{\nu_2} = 0 \qquad (21)$$

where $[OH^-]_{\nu_2}$ is the half-saturating concentration of OH^-. On the other hand, Eq. 16a provides the following equation for the lifetime (τ) of the CL

$$(k_4 + k_5[OH^-])^{-1} = \tau. \qquad (22)$$

Equation 21 and 22 can be solved together with respect to k_4 and k_5

$$k_4 = \frac{[OH^-]_{1/2}}{2[OH^-]_{1/2}\tau_{[OH^-]_{1/2}}} \qquad (23)$$

$$k_5 = \frac{1}{2[OH^-]_{1/2}\tau_{[OH^-]_{1/2}}} \qquad (24)$$

where $\tau_{[OH^-]_{1/2}}$ is the CL lifetime under the half-saturating OH^- concentration. Half-saturating OH^- concentration was determined from Fig. 4A: $[OH^-]_{1/2} = 1.8 \times 10^{-7}\ M$. $\tau_{[OH^-]_{1/2}}$ was determined from Fig. 4B: $\tau_{[OH^-]_{1/2}} = 75$ s. The rate constant obtained from the system of Eqs. 23 and 24 were: $k_4 = 6.7 \times 10^{-3}\ s^{-1}$ and $k_5 = 3.72 \times 10^3\ M^{-1}s^{-1}$. For convenience all of the rate constants, as well as the quantum yields involved in the proposed mechanism 1, are collected in Table 1.

Table 1. Quantitative parameters of the mechanism 1 describing optically pumped CL of IAA

Parameter	Reference
$k_1 = 8.79 \times 10^3\ M^{-1}\ cm^{-1}$	Present paper
$k_2 = 2.5 \times 10^5\ s^{-1}$	Present paper
$k_3 = 2.5 \times 10^9\ M^{-1}\ s^{-1}$	Present paper
$k_4 = 6.7 \times 10^{-3}\ s^{-1}$	Present paper
$k_5 = 3.72 \times 10^3\ M^{-1}\ s^{-1}$	Present paper
$\xi = 0.8$	26
$\varphi = 1.9 \times 10^{-9}$	Present paper

Nature of X

Free radical or hydroperoxide intermediates that are formed during IAA oxidation could be a substance X, which is responsible for optically pumped CL. The following types of free radicals were documented to be formed during the reaction: radical cation of IAA (14–16), scatol radical, peroxyl radicals (8,13–16) and superoxide anion radical (13). Organic hydroperoxide is formed during a free radical chain reaction accompanying enzymatic and probably photochemical IAA oxidation (7,12,17).

Identification of X requires (1) comparison of the kinetic

traces of decay of all the radical and hydroperoxide intermediates with the trace of the CL; thus intermediates with kinetic traces similar to that of the CL can be considered to be responsible for the CL and (2) changing the relative yield of suspected intermediates and monitoring the influence of the changes on the CL kinetics and spectra.

Time-resolved measurements of the concentrations of free radicals in the above system is a very complex but resolvable problem. The EPR technique can be employed for this purpose. The concentration of X under standard experimental conditions (see Materials and Methods) can be estimated using Eq. 11: $[X]_o = 2.5 \times 10^{-6}$ *M*. Free radicals of this concentration can be measured using spin traps or EPR apparatus with signal accumulation. Moreover, the concentration of X can be easily increased by increasing the rate of irradiation fluence employing, for example, a laser instead of a lamp as an irradiation source.

The problem, which cannot be presently solved is the measurement of the hydroperoxide concentration. The appropriate technique is not available. There is certain optimism that this problem will be resolved using a peroxidase/phenols system for indirect measurement of hydroperoxide concentration (28).

REFERENCES

1. Kuschnir, K. and T. Kuwana (1969) Photosensitized chemiluminescence of luminol, 6-aminophthalazine-1,4(2*H*,3*H*)-dione. *Chem. Commun.* 193.
2. Matheson, I. B. C. and J. Lee (1970) The dye-sensitized photooxidation chemiluminescence of luminol. *Photochem. Photobiol.* **12**, 9–16.
3. Matheson, I. B. C. and J. Lee (1976) The non-chemiluminescent reaction of luminol with singlet oxygen. *Photochem. Photobiol.* **24**, 605–607.
4. Motsenbocker, M., T. Sugawara, M. Shintani, H. Masuya and K. Kondo (1993) Establishment of the optically pumped chemiluminescent technique for diagnostics. *Anal. Chem.* **65**, 403–408.
5. Davies, P. J. (1995) The plant hormones: their nature, occurrence and functions. In *Plant Hormones: Physiology, Biochemistry and Molecular Biology* (Edited by P. J. Davies), pp. 4–5. Kluwer Academic.
6. Bandurski, R. S., J. D. Cohen, J. Slovin and D. M. Reinecke (1995) Auxin biosynthesis and metabolism. In *Plant Hormones: Physiology, Biochemistry and Molecular Biology* (Edited by P. J. Davies), pp. 39–65. Kluwer Academic.
7. Krylov, S. N. and H. B. Dunford (1996) Evidence for a free radical chain mechanism in the reaction between peroxidase and indole-3-acetic acid at neutral pH. *Biophys. Chem.* **58**, 325–333.
8. Kobayashi, S., K. Sugioka, H. Nakano, M. Nakano and S. Tero-Kubota (1984) Analysis of the stable end products and intermediates of oxidative decarboxylation of indole-3-acetic acid by horseradish peroxidase. *Biochemistry* **23**, 4589–4597.
9. Krylov, S. N., S. M. Krylova and L. B. Rubin (1993) Threshold effect of caffeic acid on peroxidase-catalysed oxidation of indole-3-acetic acid. *Phytochemistry* **33**, 9–12.
10. Krylov, S. N., S. M. Krylova, I. G. Chebotarev and A. B. Chebotareva (1994) Inhibition of enzymatic indole-3-acetic acid oxidation by phenols. *Phytochemistry* **36**, 263–267.
11. Krylov, S. N., B. D. Aguda and M. L. Ljubimova (1995) Bistability and reaction thresholds in the phenol-inhibited peroxidase-catalyzed oxidation of indole-3-acetic acid. *Biophys. Chem.* **53**, 213–219.
12. Krylov, S. N. and H. B. Dunford (1996) Detailed model of the peroxidase-catalyzed oxidation of indole-3-acetic acid at neutral pH. *J. Phys. Chem.* **100**, 913–920.
13. Mottley, C. and R. P. Mason (1986) An electron spin resonance study of free radical intermediates in the oxidation of indole acetic acid by horseradish peroxidase. *J. Biol. Chem.* **261**, 16860–16864.
14. Candeias, L. P., L. K. Folkes, M. F. Dennis, K. B. Patel, S. A. Everett, M. R. L. Stratford and P. Wardman (1994) Free-radical intermediates and stable products in the oxidation of indole-3-acetic acid. *J. Phys. Chem.* **98**, 10131–10137.
15. Candeias, L. P., L. K. Folkes, M. Porssa, J. Parrick and P. Wardman (1995) Enhancement of lipid peroxidation by indole-3-acetic acid and derivatives: substituent effect. *Free Radical Res.* **23**, 403–418.
16. Candeias, L. P., L. K. Folkes, M. Porssa, J. Parrick and P. Wardman (1996) Rates of reaction of indoleacetic acids with horseradish peroxidase compound I and their dependence on the redox potentials. *J. Phys. Chem.* (In press)
17. Nakajima, R. and I. Yamazaki (1979) The mechanism of indole-3-acetic acid oxidation by horseradish peroxidases. *J. Biol. Chem.* **254**, 872–878.
18. Dunford, H. B. (1993) Peroxidase catalyzed electronic excitation in Brasil and Canada. Isobutyraldehyde and indole-acetic acid. The importance of the initiation step. *Quim. Nova* **16**, 350–353.
19. Miyoshi, N., M. Fukuda and G. Tomita (1986) Flavin mononucleotide-sensitized photooxidation of indoleacetic acid. *Photobiochem. Photobiophys.* **11**, 57–65.
20. Gorman, A. A., G. Lovering and M. A. J. Rodgers (1979) The entropy-controlled reactivity of singlet oxygen ($^1\Delta_g$) toward furans and indoles in toluence. A variable-temperature study by pulse radiolysis. *J. Am. Chem. Soc.* **101**, 3050–3054.
21. Cilento, G. (1980) Photobiochemistry in the dark. *Photochem. Photobiol. Rev.* **5**, 109–228.
22. Cilento, G. (1984) Generation of electronically excited triplet species in biochemical systems. *Pure Appl. Chem.* **56**, 1179–1190.
23. Krylov, S. N. and A. B. Chebotareva (1993) Peroxidase-catalyzed co-oxidation of indole-3-acetic acid and xanthene dyes in the absence of hydrogen peroxide. *FEBS Lett.* **324**, 6–8.
24. Krylov, S. N., V. V. Lazarev and L. B. Rubin (1990) Kinetics associated with chemiluminescence spectra during the oxidation of heteroauxin by peroxidase. *Dokl. Biophys.* **310**, 28–31.
25. De Melo, M. P., J. A. Escobar, D. Metodiewa, H. B. Dunford and G. Cilento (1992) Horseradish peroxidase-catalyzed aerobic oxidation of indole-3-acetic acid. *Arch. Biochem. Biophys.* **296**, 34–39.
26. Neckers, D. C. and O. M. Valdes-Aguilera (1993) Photochemistry of the xanthene dyes. *Adv. Photochem.* **18**, 315–394.
27. Robinson, J. and J. M. Cooper (1970) Method of determining oxygen concentration in biological media, suitable for calibration of the oxygen electrode. *Anal. Biochem.* **33**, 390–399.
28. Krylov, S. N. and H. B. Dunford (1996) Detailed mechanism of phenol-inhibited, peroxidase-catalyzed oxidation of indole-3-acilic acid at neutral pH. *Photochem. Photobiol.* (In press).